

To appear in “Ringberg Workshop on Large-Scale Structure”,
ed. D. Hamilton (Kluwer, Amsterdam)

TOWARD HIGH-PRECISION MEASURES OF LARGE-SCALE STRUCTURE

MICHAEL S. VOGLEY¹
Princeton University Observatory
Peyton Hall, Princeton, NJ 08544
vogeley@astro.princeton.edu

Abstract. I review some results of estimation of the power spectrum of density fluctuations from galaxy redshift surveys and discuss advances that may be possible with the Sloan Digital Sky Survey. I then examine the realities of power spectrum estimation in the presence of Galactic extinction, photometric errors, galaxy evolution, clustering evolution, and uncertainty about the background cosmology.

1. INTRODUCTION

The advent of deep redshift surveys of $10^4 - 10^6$ galaxies, such as the Las Campanas Redshift Survey (LCRS; Shectman *et al.* 1996) and the AAT 2df survey (Colless 1998), and multiband photometric and spectroscopic surveys such as the Sloan Digital Sky Survey (SDSS; Gunn & Weinberg 1995; Szalay 1998), marks the beginning of a new era of investigations in large-scale structure. Rather than treat galaxies as indistinguishable tracers of mass in a static distribution, we will study the detailed dependence of clustering on galaxy type and cosmic epoch. In fact, as I will discuss, we must study the species and redshift dependence of clustering to precisely differentiate among cosmological models. In somewhat shallower wide-angle surveys (Huchra *et al.* 1983; Giovanelli & Haynes 1984; Geller & Huchra 1989; da Costa *et al.* 1994; Fisher *et al.* 1995) it has been possible to begin study of these effects; at redshift $z = 0.1$ and larger it becomes critical to do so. In addition to precisely characterizing galaxy clustering at the present epoch, we will use the anisotropy of clustering, as well as the evolution of this clustering, to constrain cosmological parameters.

¹Hubble Fellow

A key issue that I examine is the limiting precision with which we can hope to measure galaxy clustering at the present epoch. Although much has been made of the power of large galaxy surveys to measure cosmological parameters, most of this discussion has focussed on finding an analysis method that gives “optimal” uncertainties on model parameters, where the uncertainties are due to cosmic variance and shot noise (Vogeley & Szalay 1996; Tegmark *et al.* 1998). Much less has been said about the uncertainties caused by random and systematic errors in photometry or Galactic extinction corrections, and systematic uncertainties that arise from issues of cosmology, and evolution of galaxies and their clustering. In this paper I discuss the impact of these effects on analysis of galaxy redshift samples from the SDSS.

2. MEASUREMENTS OF THE POWER SPECTRUM FROM GALAXY SURVEYS

Rather than give a review of the myriad measures of galaxy clustering that we hope to apply to these new surveys, here I focus on one statistic and examine how possible random and systematic uncertainties will affect the accuracy of this measurement. Not surprisingly, I consider the power spectrum of galaxy density fluctuations, because lowest-order measures are where we first gain precision, and because uncertainties in higher-order measures often scale from the uncertainties in the variance.

2.1. THE DATA

Figure 1 plots the power spectrum $P(k)$ in units of $h^{-3} \text{ Mpc}^3$ (a power spectral density) as estimated from a number of radio (Peacock & Nicholson 1991), infrared (Fisher *et al.* 1993; Tadros & Efstathiou 1995), and optically-selected (da Costa *et al.* 1994; Lin *et al.* 1995) galaxy redshift survey samples, and the real-space power spectrum inferred from angular clustering of a photometric sample (Baugh & Efstathiou 1993). To avoid hopelessly confusing the plot, no error bars are shown (unfortunately, the various authors differ somewhat in their choice of binning and methods of computing these uncertainties, so comparison of these errors would not be as informative as one might hope). The shapes of most of these spectra roughly agree over the decade $10 - 100h^{-1} \text{ Mpc}$. However, there is large variation of their amplitudes. We usually attribute this variation to differences in the “bias parameter,” which affects the amplitudes as $P_1(k)/P_2(k) = (b_1/b_2)^2$ if the bias is scale-independent. This strong dependence of clustering amplitude on method of galaxy selection implies that detailed knowledge of the selection criteria and construction of sub-samples for analysis that are homogeneous in this selection are prerequisites for precision measurement

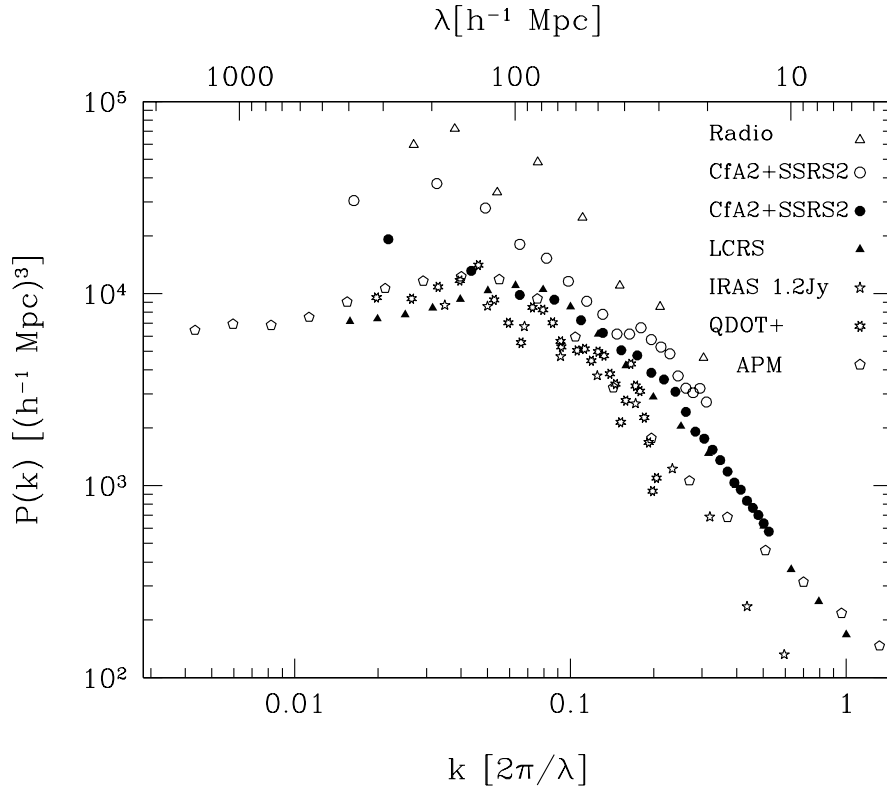


Figure 1. Estimates of the redshift-space power spectrum from a variety of redshift surveys, and an estimate of the real-space power spectrum inferred from angular correlations (APM).

of the power spectrum.

To clarify comparison of the shapes of the power spectra, Figure 2 plots these same data, with the amplitudes of the curves shifted so that all match $P(k)$ of the LCRS sample near wavenumber $k = 0.1$. No shift was required to obtain agreement between the LCRS and the CfA2+SSRS2-100 volume-limited sample, which is not surprising since they both include optically-selected galaxies that are roughly M^* and brighter. In general, one sees excellent agreement between optical redshift samples for wavenumbers $k > 0.1$. There is some disagreement between infrared and optical samples over this same range of wavenumber, perhaps because the selected galaxies sample different physical environments. One should be careful not to

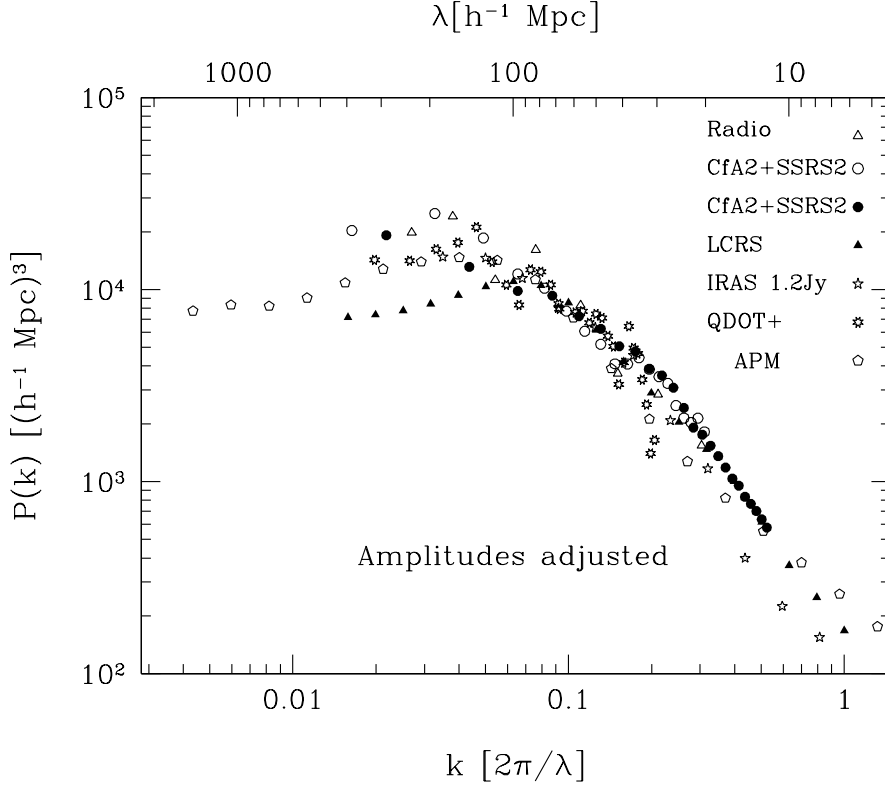


Figure 2. Power spectrum estimates from Figure 1 arbitrarily scaled to match at $k = 0.1$ to allow comparison of power spectrum shapes. CfA2+SSRS2-101 and LCRS were not adjusted.

over-interpret this comparison of spectral shapes. Where large shifts are necessary to match the amplitudes, this shifting procedure is questionable, because the effects of redshift distortions (both the linear boost described by Kaiser 1987 and the washing out of small-scale power due to redshift fingers of clusters) and non-linear evolution both depend on the ratio of galaxy-clustering to mass-clustering amplitude. On large scales, at wavenumber $k < 0.1$, we find significant departures in the shapes of the spectra, with a scatter of roughly a factor of three among the samples. This scatter is consistent with the uncertainty due to cosmic variance (small sample volume relative to the wavelength scales of interest).

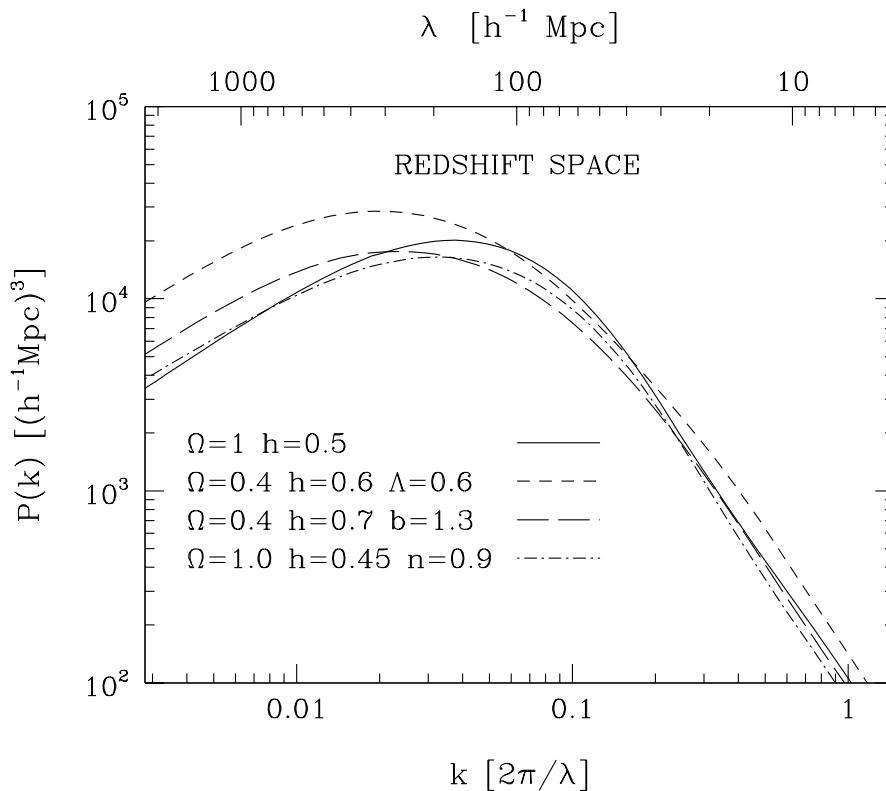


Figure 3. Non-linear redshift-space power spectra for a variety of COBE-normalized CDM models.

2.2. MODEL FITS

The shape of these spectra may be well-fitted by a linear Cold Dark Matter (CDM) power spectrum (Bardeen *et al.* 1986) with shape parameter $\Gamma = 0.25$ (where $\Gamma = \Omega h$ in the simplest models, with $h = H_0/100$). Here we use the linear CDM spectrum merely as a fitting function. It is interesting to note that, for values of $\Gamma = \Omega h \sim 0.25$, this linear curve does a reasonable job in fitting the redshift-space power spectrum of a fully non-linear evolved CDM model because the effects of non-linear evolution and redshift distortion nearly cancel out.

Does this fit to the spectral shape imply that our work is done? Hardly. This rough shape might be matched by tweaking the parameters of several

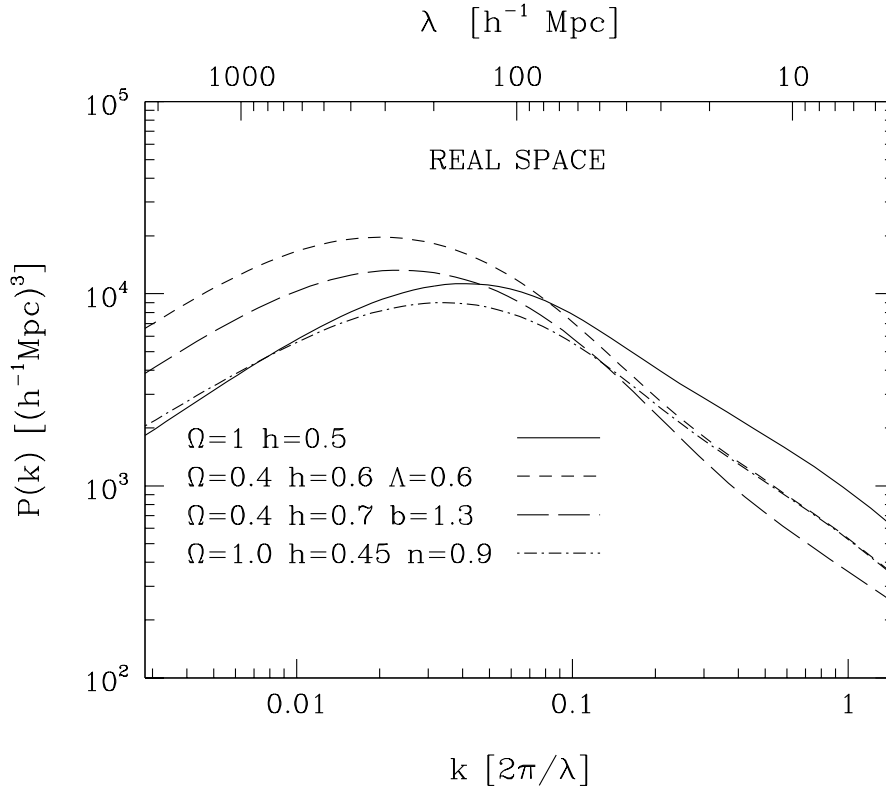


Figure 4. Real-space power spectra for the same models plotted in Figure 3.

competing models (*e.g.*, by adding some cosmic density in neutrinos and/or by varying the slope of the primordial power spectrum). We require higher resolution to detect features in the power spectrum that might be caused by acoustic oscillations near recombination (Eisenstein & Hu 1998) or other physical effects. Higher resolution in the Fourier domain requires a larger survey volume (see next section), which is also necessary to probe large wavelength scales. Measurements of the power spectrum to accuracies of a few percent on scales $\lambda > 100h^{-1}\text{Mpc}$ would allow detailed comparison of clustering of galaxies at the present epoch with clustering of the mass at redshift $z = 10^3$, as revealed by the anisotropy of the Cosmic Microwave Background (CMB).

Figure 3 illustrates how CDM models with different parameters yield

redshift-space power spectra that are similar. To compute these spectra, I use the semi-analytic formalism described by Peacock (1997) to approximate the effects of non-linear gravitational evolution and redshift distortions on the linear CDM spectrum. All of these models have a mass spectrum that is normalized to match the COBE DMR measurement of the CMB anisotropy (Wright *et al.* 1996). Even without exploring admixtures of CDM and neutrinos (*e.g.*, Primack *et al.* 1995), we see that several choices of parameters might fit the equally well (or equally poorly, depending on one’s taste). Not examined here is how the small-scale power spectrum depends on the details of galaxy formation relative to the mass distribution.

2.3. REAL VS. REDSHIFT SPACE

One of the problems of working in redshift space is that a large amount of small-scale power creates a large small-scale velocity dispersion. In redshift space, the resulting “fingers of God” wash out much of this same small-scale power. Similarly, for fixed normalization and Hubble constant, CDM models with large Ω experience a significant boost of their redshift-space power spectrum amplitudes (1.87 if $\Omega = 1$ and $b = 1$), which makes their large-scale spectra look more like those of low Ω models.

Redshift-space power spectrum measurements with accuracy of a few percent could differentiate between the model spectra in Figure 3 but, clearly, it would be easier to break the model degeneracy that we see in redshift-space power spectra if we could access the underlying real-space (*i.e.*, configuration space) power spectrum of the galaxy distribution. Figure 4 shows the power spectra of the same models from Figure 3, now plotted in real space.

The lesson here is not that we should use the angular correlation function, and give up measuring redshifts, but rather that we should take advantage of the anisotropy of clustering in redshift space to allow measurement of both the power spectrum and Ω . Andrew Hamilton’s contribution to this volume examines this issue in great detail.

3. MINIMAL POWER SPECTRUM UNCERTAINTIES FOR THE SDSS

Power spectrum measurements with accuracy of a few percent on scales from one to a few hundred Mpc would allow us to make great strides in constraining cosmological models. Is this feasible? Here I begin to examine the accuracy with which we dare hope to measure $P(k)$ in the foreseeable future.

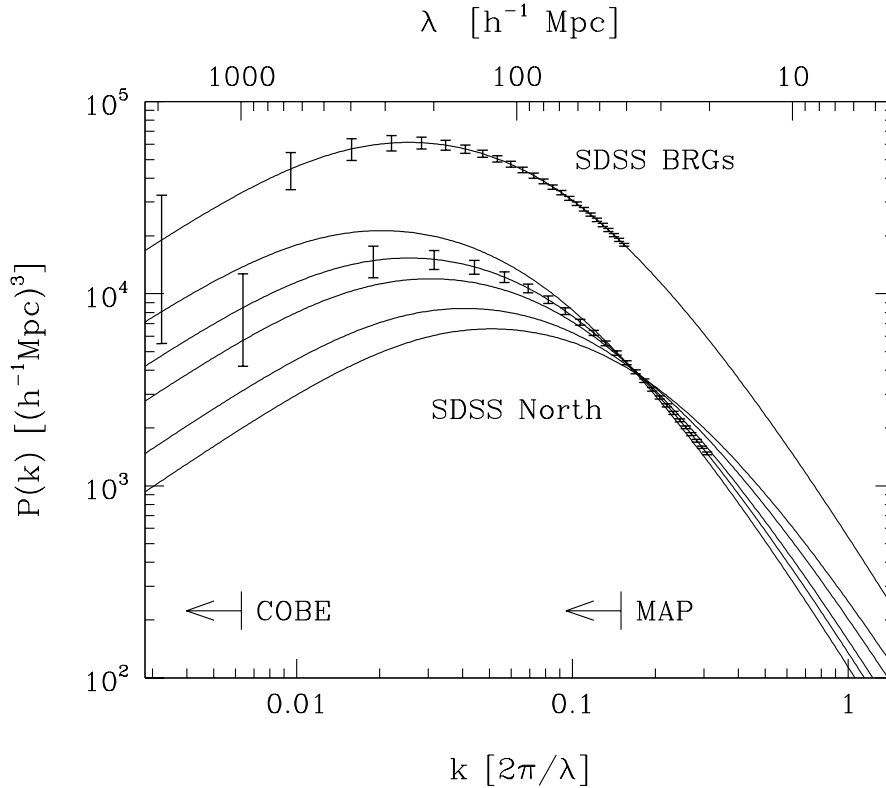


Figure 5. Predicted uncertainties in the power spectrum estimated from a volume-limited ($R_{max} = 500h^{-1}$ Mpc) sample of SDSS North and for the Bright Red Galaxy sample (upper set of error bars). These errors assume that the true power spectrum is that of an $\Omega h = 0.25$ CDM model and that the BRGs are more clustered than normal galaxies. Plotted for comparison to the SDSS North errors are CDM power spectra (normalized to $\sigma_8 = 1$) for a range of Ωh from 0.2 (uppermost curve) to 0.5 (lowest curve) and indications of the range of comoving scales probed by the COBE and MAP CMB anisotropy experiments.

3.1. APPROXIMATE UNCERTAINTY PREDICTIONS

For fixed survey strategy, the survey volume and the number density of galaxies in the redshift sample set a lower bound on the uncertainty in the estimated power spectrum. In the limit of a perfectly spherical volume-

limited sample, the uncertainty in the estimated power per mode is roughly

$$\frac{\delta\tilde{P}(k)}{\tilde{P}(k)} \approx \sqrt{2\frac{V_c}{V_k}} \left[1 + \frac{S(k)}{P(k)} \right] \quad (1)$$

(Feldman, Kaiser, & Peacock 1994). $P(k)$ and $\tilde{P}(k)$ are the true and estimated power spectra, respectively. $S(k) = 1/\bar{n}$ is the shot noise power for mean galaxy density \bar{n} . $V_c = (2\pi)^3/V_S$ is the coherence volume in the Fourier domain for a survey with volume V_S . It is assumed that we average the power estimates over a shell in Fourier space with volume $V_k \approx 4\pi k^2 \Delta k$. That is, we average the power over all angles, and over bins with width $\Delta k > 2\pi/R$, where R is the survey depth. For a larger volume, the coherence volume in Fourier space decreases, thus we obtain a larger number of independent probes of the power spectrum. This convenient approximation breaks down when the survey volume is highly anisotropic; in this case the coherence volume in Fourier space (the “window function”) becomes anisotropic and the range of true wavenumber that is probed depends on the direction of \mathbf{k} . Figure 8 of Alex Szalay’s contribution to this volume shows window function shapes and relative sizes for a variety of redshift surveys, including the SDSS.

A volume-limited sub-sample of the SDSS redshift survey in the North Galactic Cap region (this covers solid angle of π steradians) that has comoving coordinate depth of $R = 500h^{-1}$ Mpc will include all galaxies with absolute magnitude roughly 0.4^m brighter than M^* , with mean number density $\bar{n} \sim 2 \times 10^{-3} h^3 \text{Mpc}^{-3}$. Hereafter I will use this as a fiducial sample for computing uncertainties in the estimated power spectrum. This sample is conservative, in the sense that the SDSS will allow selection of much deeper samples, which include more volume, and because a magnitude-limited sample to the same depth would have larger average number density, hence smaller shot noise.

Figure 5 plots 1σ uncertainties for power estimates binned by $\Delta k = 2\pi/(500h^{-1}\text{Mpc})$ and assuming that the true power spectrum is described by a $\Gamma = 0.25$ linear CDM spectrum. Also shown are a family of CDM spectra with different shape parameter Γ . The uncertainty in each bin of width Δk at a wavelength scale of $\lambda = 100h^{-1}\text{Mpc}$ will be $\sigma(\hat{P})/\hat{P} \approx 0.06$. Such a measurement would easily differentiate between various CDM models, as the family of CDM curves indicates. Comparison with results from the LCRS further illustrates the power of such a large survey: if a “bump” at $\lambda \sim 128h^{-1}\text{Mpc}$ were found in the SDSS sample with $\delta\hat{P}/\hat{P}_{smooth} = 0.76$ in a single bin (as seen by Landy *et al.* 1996), this would be a 12σ event.

3.2. SAMPLES WITH LARGER VOLUME?

Could we do better than the SDSS with, for example, an all-sky survey to similar depth? This suggestion is not out of the question, if we combine all of the redshift surveys that will exist in a few years' time. The SDSS NGP survey will cover one quarter of the sky; a similar full-sky survey would have power spectrum uncertainties that are at best a factor of two smaller. More realistic at optical wavelengths would be a survey over Galactic latitude $|b| > 30$, which covers half the sky, yielding errors that are at best 40% smaller than the SDSS. In fact, the SDSS itself will cover an effective area larger than π steradians, by including three slices in the southern Galactic hemisphere, each $3^\circ \times \sim 100^\circ$ in area. If the SDSS is combined with the AAT 2df redshift survey and the LCRS, then most of the high-latitude sky will be sampled. Galaxy selection in the infrared would allow a true full-sky survey, but no IR photometric survey exists to depth comparable to the SDSS. The IRAS PSC-Z survey (Saunders *et al.* 1994) comes closest to this goal, but has much larger shot noise (smaller galaxy density) and apparently more severe sample evolution.

One-tenth of the million galaxies targeted for spectroscopy by the SDSS will be a sample of Bright Red Galaxies (BRGs) that are volume-limited to redshift $z = 0.45$. The volume limit will be enforced by selecting the galaxies by their absolute magnitudes, estimated using the photometric redshift technique (Connolly *et al.* 1995). This sample will cover a volume eight times larger than the fiducial SDSS-500 sample described above, albeit with larger shot noise. The upper curve and error bars in Figure 5 show the expected uncertainties from cosmic variance and shot noise in the SDSS BRG sample, using equation 1 and assuming that the BRGs are biased by a factor of 2 (factor of 4 in the power spectrum) relative to the normal galaxy sample. The brightest and reddest galaxies appear to evolve least of all, so this sample will provide our best chance to measure the evolution of clustering (see section 5.3 below).

4. MEASUREMENT ERRORS AND EXTERNAL SYSTEMATICS

In the previous section I describe “ideal” uncertainties that are lower bounds on the total error budget. I now examine whether these expectations are realistic. What other effects limit our knowledge of clustering at the present epoch? I use the SDSS as a test case, but the following analysis is also relevant for other surveys to similar depth.

There are several possible effects about which we do not need to worry for the SDSS. Because the galaxies in the spectroscopic sample will be five magnitudes brighter than the point source detection limit, star-galaxy

separation will not be a problem. Galaxies with very low central surface brightness will be excluded from the redshift sample, because we would not be able to get redshifts of these objects, but we will understand this selection bias quite well. For example, our magnitude and surface brightness cuts will be “fuzzy,” such that we observe some fraction of objects beyond the nominal cuts. The redshifts that we do measure will have $20 - 30 \text{ km s}^{-1}$ accuracy, so this project is overkill for simply measuring redshifts and we expect very few failures. The use of a fiber-fed spectrograph with plugplates to hold the fibers in the focal plane imposes a 55 arcsecond minimum separation for pairs of objects, except where a target lies in the overlap between two or more plugplate fields. However, during the Fall observing season, the larger ratio of spectroscopic time to photometric time (because we will image a smaller area), will allow a larger covering factor for spectroscopy, thus we will obtain spectra for at least all pairs of objects and potentially could observe all n-tuples up to $n = 7$. From these southern data, we will study the effects of excluding close pairs from the northern spectroscopy (*e.g.*, we can study the very small-scale velocity dispersion of galaxies from the southern spectroscopy).

4.1. EFFECTS OF EXTINCTION AND PHOTOMETRIC ERRORS

Despite our best efforts at correcting for Galactic extinction and calibrating the photometry, errors in these will add to the minimal uncertainties illustrated in Figure 5. In collaboration with Andy Connolly at Johns Hopkins, I have investigated the impact of such errors on power spectrum estimation from samples of the SDSS (Vogeley & Connolly 1998). The remainder of this section is an overview of some of our results.

Errors in either photometry or the extinction corrections affect the apparent number density of galaxies in similar fashion. Here we consider only the effects of extinction or photometric error on total magnitude selection. Although the SDSS spectroscopic samples will also be chosen on the basis of a central surface brightness cut, simulations of the SDSS indicate that surface brightness dimming from extinction will affect an insignificant number of galaxies.

In a volume-limited sample that should include all galaxies brighter than absolute magnitude M_{lim} , a magnitude error of Δm over a patch on the sky causes the apparent galaxy density in that direction to differ from the true galaxy density by

$$\begin{aligned} \frac{n_{obs}}{n_{true}} &= \frac{\Phi[< M - \Delta m]}{\Phi[< M]} \\ &\approx 1 - \frac{\phi(M)\Delta m}{\Phi[< M]} \end{aligned} \quad (2)$$

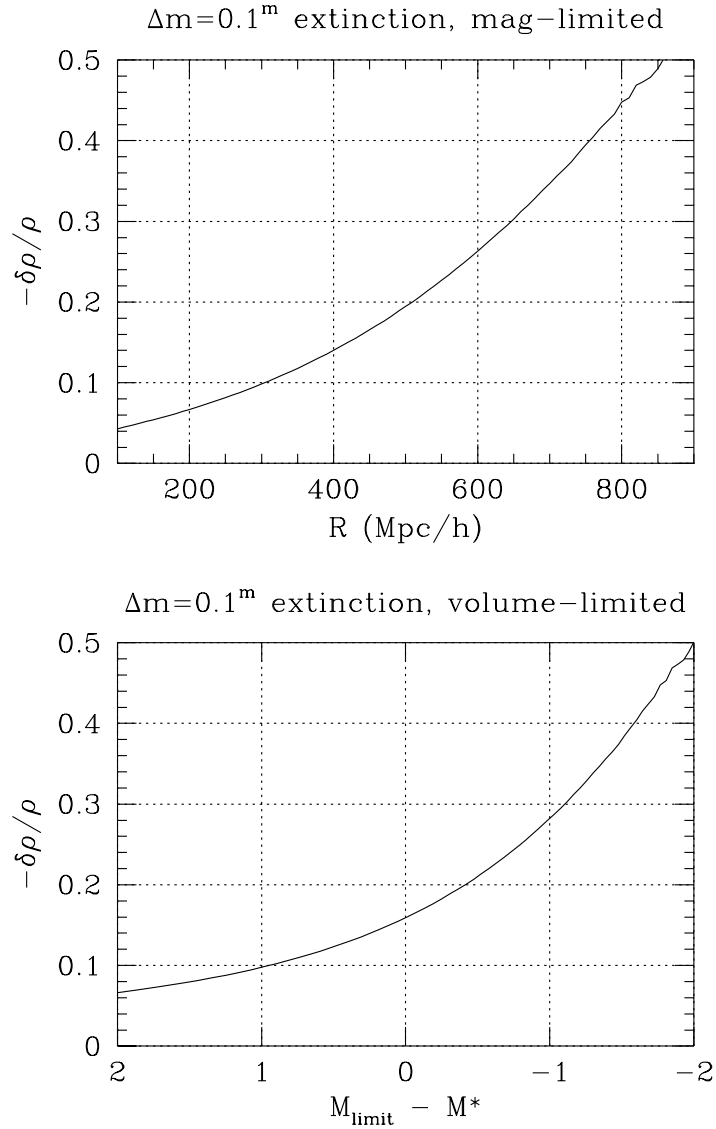


Figure 6. Effects on the observed galaxy density that would result from 0.1^m of extinction in a magnitude-limited (upper panel) or volume-limited (lower panel) redshift sample of the SDSS.

$$\sim \exp \left[-\Delta m 10^{0.4(M^* - M_{\text{lim}})} \right],$$

where $\phi(M)$ and $\Phi(< M)$ are the differential and integrated luminosity

functions of the galaxies. The approximations are valid for a Schechter luminosity function when M_{lim} is close to or brighter than M^* . This form clearly shows how the strength of the effect depends on the slope of the luminosity function near the magnitude limit; deeper sub-samples will be more severely affected by extinction or photometric uncertainty than shallow samples because the count slope is steeper. For a magnitude-limited sample with limit m_{lim} , the absolute magnitude limit varies with distance $M_{lim}(r)$ and the apparent density differs from the true galaxy density by

$$\frac{n_{obs}}{n_{true}} = \frac{\Phi[< M(r) - \Delta m]}{\Phi[< M(r)]}. \quad (3)$$

Figure 6 shows the effect of a $\Delta m = 0.1^m$ error on the apparent density of volume-limited and magnitude-limited samples of the SDSS. This modulation of the apparent density grows with distance in a magnitude-limited sample and is, on average, less severe than in an volume-limited sample that is cut off at the same depth. In the following analysis I consider volume-limited samples because (1) the effects are more severe for these, thus the analysis is conservative in the sense of giving worst-case errors and (2) we won't believe the results of magnitude-limited power spectrum analyses until we understand how the clustering amplitude differs among galaxy species (see section 2.1 above).

4.2. THE POWER SPECTRUM OF GALACTIC EXTINCTION

Because Galactic extinction modulates the apparent density of galaxies, it could cause erroneous clustering power to appear in our data. To leading order, the net effect is to add to the apparent clustering, $P_{obs}(k) \approx P_{true}(k) + P_{extinction}(k)$. If we make no correction at all for Galactic extinction, we expect to observe extra clustering power in the SDSS-500 sample, as shown in Figure 7. Here we predict the effect of extinction over the SDSS North region using a cosecant law, the Burstein & Heiles (1982) map, and the Stark *et al.* (1992) HI map. These maps predict similar clustering power; it is the large-scale cosecant-like variation in extinction that causes the trouble. Restricting the analysis to somewhat higher Galactic latitude ($|b| > 40^\circ$) only slightly ameliorates the problem. Failure to notice that we live in a Galaxy that is laced with dust would cause one to infer that the power spectrum of the universe suddenly rises in power-law fashion beyond $200 - 300h^{-1}$ Mpc.

Fortunately, we are not oblivious to the effects of dust and we plan to make some correction for this effect. The SDSS will select spectroscopic targets after applying an *a priori* correction for extinction to the apparent magnitudes, thus constructing a sample that is uniform in an extragalactic sense. As of this date we plan to use the extinction maps that have

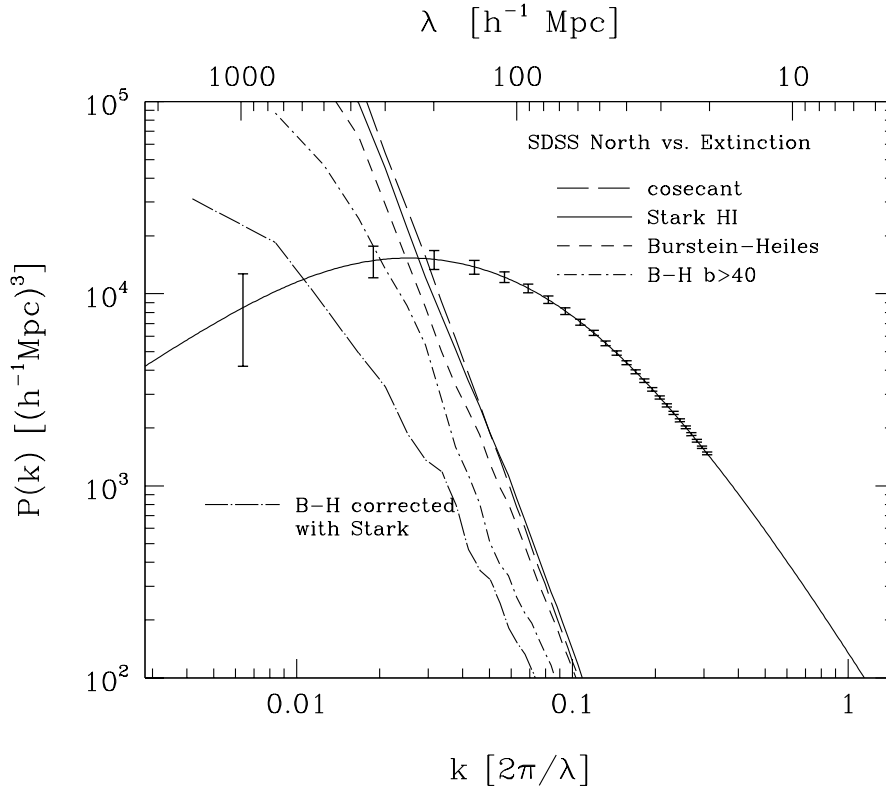


Figure 7. False observed clustering power that would be caused by Galactic extinction, for different assumed extinction maps. For comparison is an $\Omega h = 0.25$ CDM power spectrum and the expected uncertainties for a volume-limited sample of SDSS North. If we make no correction for extinction, then the false clustering power exceeds the true power for $\lambda \gtrsim 300h^{-1}$ Mpc. Cutting back the edges of the survey to $b > 40^\circ$ has only a small effect. If we correct the B&H map using a crudely-calibrated map derived from the Stark *et al.* HI maps, the residual power exceeds the true power for scales $\lambda \gtrsim 700h^{-1}$ Mpc.

been constructed from the DIRBE and IRAS satellite data by Schlegel, Finkbeiner, & Davis (1998). If we or others later construct a better extinction map, we will take the residuals into account when we analyze the data. The erroneous clustering power that we really need to worry about is caused by unknown residuals between our best extinction map and the true Galactic extinction.

The lower dot-dashed line in Figure 7 shows what happens if the true

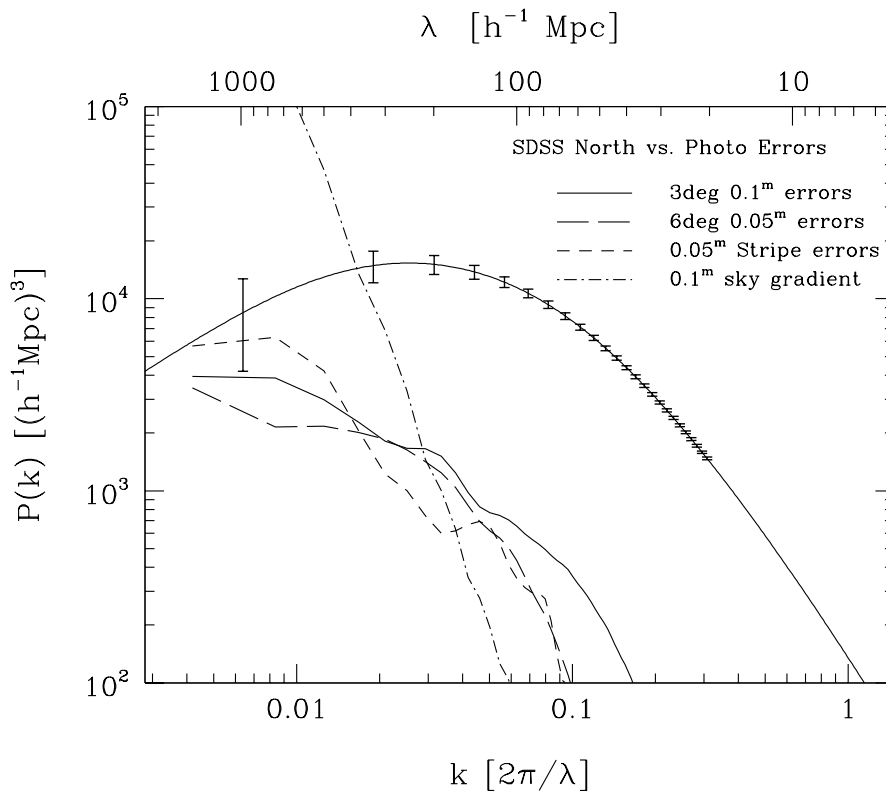


Figure 8. False clustering power due to fluctuations of the photometric zeropoint (or errors in the extinction map) on 3° and 6° scales, or between stripes of the SDSS. Also shown is the effect of a 0.1^m gradient across the sky.

extinction is described by the Burstein-Heiles map and we use a crudely-calibrated (here we applied our own *ad hoc* dust-to-gas relation) version of the Stark *et al.* HI map to estimate and correct for the extinction. Even with this roughly calibrated map, the extinction power is below the true power on scales smaller than $700h^{-1}\text{Mpc}$. A well-calibrated map would allow us to accurately probe the entire range of accessible scales.

4.3. THE POWER SPECTRUM OF PHOTOMETRIC ERRORS

Similar to the effects of extinction, errors in photometry that are correlated over a patch of sky will modulate the apparent density of galaxies. Ran-

dom (uncorrelated between galaxies) errors will contribute to the notorious Malmquist bias; here we consider only correlated photometric errors, such as those that might arise from variations in the zero point.

Figure 8 shows the extra clustering power in the SDSS-500 sample that we would observe if the photometric zero-point varies by 0.1^m over patches that are 3° in diameter (the field of view of the SDSS camera), or by 0.05^m over patches that are 6° in diameter (the size of a Schmidt plate). These curves should match on scales much larger than the patch size, but vary somewhat because we compute these curves using a Monte Carlo realization of the errors. Even such gross errors in photometry produce erroneous clustering that is less than 10% of the true power for $\lambda < 10^3 h^{-1} \text{Mpc}$.

The relatively small amplitude of power caused by even 0.1^m photometry errors over the field of view of the SDSS camera is very good news for the extinction problem. This result implies that we can cure the extinction problem if we can use the SDSS data themselves to construct an extinction map that has random field-field errors that are smaller than 0.1^m (but, of course, without any large-scale systematic errors). Variations in faint galaxy counts and colors and colors of hot Galactic halo subdwarfs offer several means for constructing such a map, which would provide an independent method for computing extinction corrections.

The lesson of the extinction errors is that large-scale gradients, rather than small-scale random photometry errors, are the real worry. Figure 8 also shows the extra clustering power that arises if there is a zero-point gradient across the sky (pole to pole) of 0.1^m or if the zero-point randomly varies by 0.05^m between the “stripes” of the SDSS. In other words, the latter illustrates what happens if the photometry is consistent within each $\sim 3^\circ \times 120^\circ$ scan region, but the calibration zero-point varies between disjoint regions. Even such a severe error (which we would no doubt notice by comparing the overlap regions of the scans) would produce extra power that is below 10% of the true power on scales $< 10^3 h^{-1} \text{Mpc}$. To be certain, we would not be happy to have a 10% effect in our measurements. The point is that this is clearly an upper bound on the magnitude of such an effect.

It is important to note that, just as examination of the anisotropy of clustering will reveal the effects of redshift distortion on the power spectrum, comparison of clustering in the angular and radial directions will provide a test of false clustering due to extinction or photometric error. Cross-correlation of the angular clustering of samples that are selected to lie at different distance would clearly reveal the signature of correlated magnitude errors.

5. EVOLUTION: THE UNIVERSE, GALAXIES, AND CLUSTERING

What is the “present epoch?” For statistical analyses of clustering, a useful definition is the redshift range beyond which ignorance of, or inability to correct for, the effects of evolution of galaxies and their clustering becomes the dominant source of uncertainty. In this section I examine how the apparent power spectrum is affected by (1) the mapping between redshift and comoving coordinate distance, (2) galaxy evolution, and (3) clustering evolution. Careful analysis will allow us to learn about evolution; the question here is, when do these effects begin to dominate the apparent clustering?

5.1. KNOW THY COSMOLOGY

The relationship between redshift and comoving coordinate distance depends on the deceleration parameter q_0 ,

$$r(z) = \frac{c}{H_0 q_0^2 (1+z)} \left[q_0 z + (1 - q_0) \left(1 - \sqrt{1 + 2q_0 z} \right) \right]. \quad (4)$$

Out to redshifts of a few thousand km s^{-1} , it matters very little which value of q_0 we use. But at larger distance, this transformation begins to affect galaxy clustering in several ways. Using the wrong q_0 will cause fluctuations on a fixed comoving scale to appear as fluctuations on different apparent scales as a function of redshift. Over the redshift range probed by the SDSS this effect would cause only minor smearing of features in the spectrum; varying q_0 from 0.1 to 0.5 changes the length scale by only 4% over the redshift range $z = 0$ to $z = 0.1$.

It also follows that the comoving volume element depends on q_0 , as

$$\frac{dV}{dz} = 2\pi \left(\frac{c}{H_0} \right)^3 \frac{[q_0 z + (1 - q_0)(1 - \sqrt{1 + 2q_0 z})]^2}{q_0^4 (1+z)^3 \sqrt{1 + 2q_0 z}}. \quad (5)$$

If we assume a value of q_0 that is too large, the volume element dV will erroneously decrease with distance, and cause a radial gradient in the apparent galaxy density. Varying q_0 from 0.1 to 0.5 raises the comoving galaxy density by 8% at redshift $z = 0.1$.

Because construction of volume-limited samples relies on using the redshift to compute the absolute magnitudes of the galaxies, an error in q_0 translates into an error in the inferred absolute magnitudes,

$$\Delta M = 5 \log \left[r(z, q_0^{\text{true}}) / r(z, q_0^{\text{assumed}}) \right]. \quad (6)$$

This error in the absolute magnitudes yields a gradient in apparent galaxy density, as described by equation 2. Using too large a value of q_0 , we would

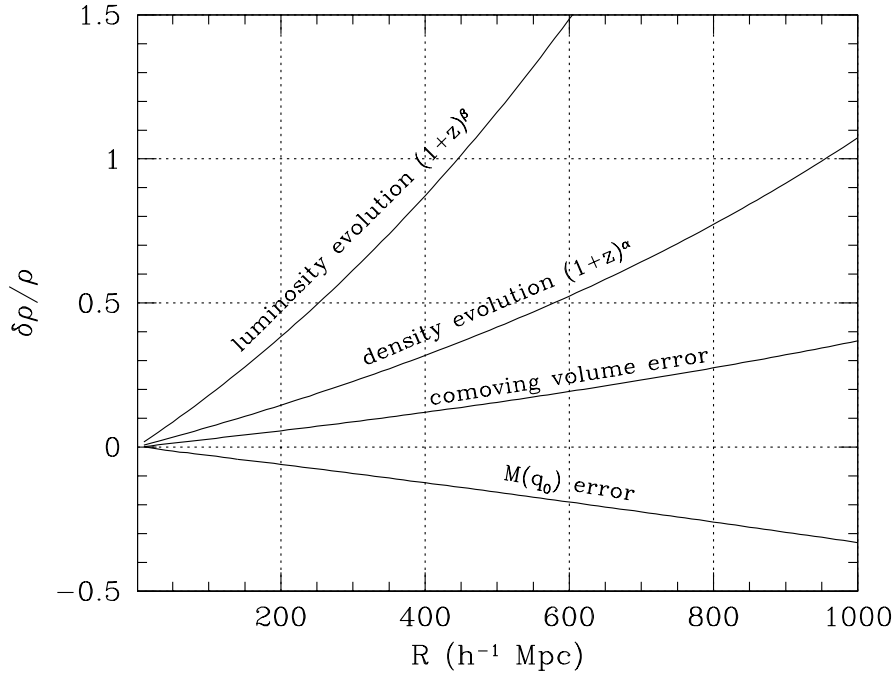


Figure 9. Density gradients caused by (from top to bottom) galaxy luminosity evolution with $\beta = 2.3$, density evolution with $\alpha = 2$, error in the computed comoving volume, and error in the computed absolute magnitudes in an absolute-magnitude limited sample of the SDSS. The latter two cosmological effects are shown for the case in which the true $q_0 = 0.1$ but we have used $q_0 = 0.5$ to relate redshifts to comoving coordinate distances.

infer that galaxies are fainter than their true luminosity and exclude some from our sample, thus lowering the galaxy density at large redshift. At redshift $z = 0.1$, varying q_0 from 0.1 to 0.5 lowers the density by 7%.

Figure 9 shows the density gradients in the SDSS-500 volume-limited sample that would result from assuming $q_0 = 0.5$ if the true value is $q_0 = 0.1$. Interestingly, the rise in apparent density that results from the change in comoving volume element nearly cancels the absolute-magnitude effect (this cancellation is not universally true because the absolute-magnitude effect depends on the slope of the integrated luminosity function at the absolute magnitude limit).

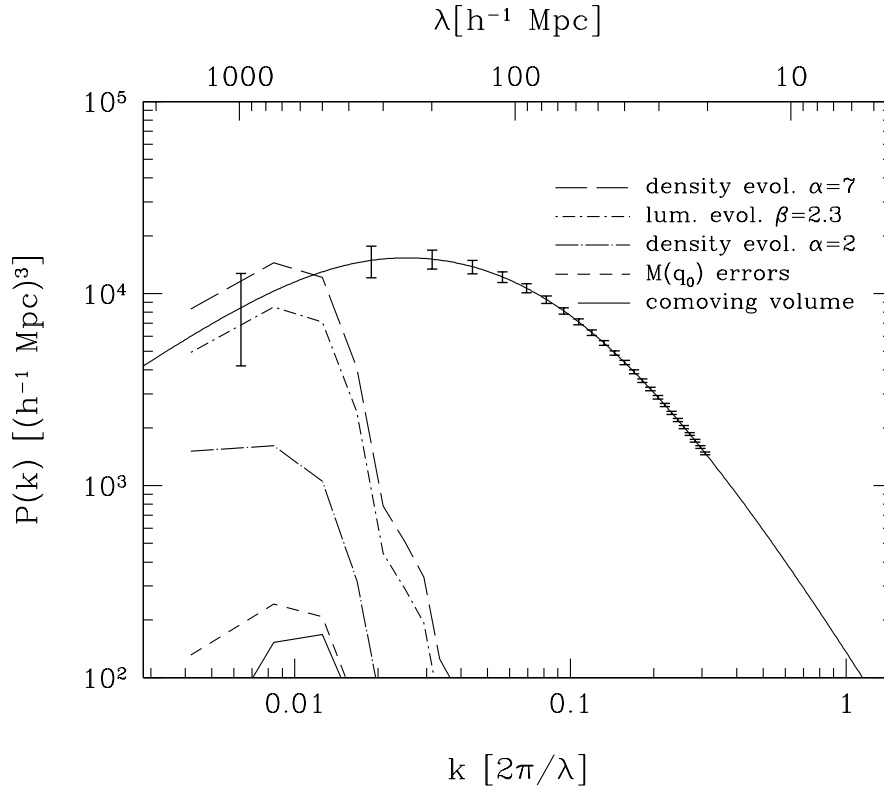


Figure 10. False clustering power that would be observed in the SDSS-500 volume-limited sample by (top to bottom) galaxy density evolution with $\alpha = 7$, galaxy luminosity evolution with $\beta = 2.3$, density evolution with $\alpha = 2$, and from gradients caused by using the wrong value of q_0 . In every case, the sharp turnover at small k is an artifact of our failure to correct for a numerical effect.

Figure 10 illustrates the extra clustering power that results from these effects, considered separately. Both the comoving volume effect and the absolute magnitude effect cause negligible power because the gradient is so shallow. Even if these gradients did not cancel, they would not be a cause for worry in samples that extend to $R = 500h^{-1}$ Mpc.

5.2. GALAXY EVOLUTION

Also shown in Figures 9 and 10 are the density gradients and extra clustering power predicted for galaxy luminosity or density evolution. Here we

model density evolution as $\bar{n}(z) \propto (1+z)^\alpha$ with $\alpha = 2$ shown in Figure 9, and both $\alpha = 7$ (upper curve) and $\alpha = 2$ (middle curve) in Figure 10. If α is much larger than 2, this effect could cause trouble in the SDSS samples. For example, Saunders *et al.* (1990) find evidence for $\alpha = 7$ in the IRAS-selected galaxy luminosity function. We model luminosity evolution as $L(z) \propto (1+z)^\beta$ with $\beta = 2.3$, as fit by Lilly *et al.* (1995) to their *I*-band luminosity functions. Saunders *et al.* find $\beta = 3$ for IRAS galaxies. Figure 10 shows that this type of luminosity evolution would contribute a significant amount of clustering power on the largest scales probed by the SDSS-500 sample.

A related effect is the difficulty of computing the K-corrections for galaxies over a large range of redshift. Out to redshift $z = 0.2$, failing to perform the proper K-corrections in r' (the selection band for SDSS spectroscopy) causes an effect on the galaxy samples that is somewhat smaller than the luminosity evolution effect.

The lesson here is that one cannot treat galaxies as indistinguishable “points” for the purpose of power spectrum analysis. We already know this from, for example, luminosity bias, whereby very bright galaxies are more strongly clustered than the average (*e.g.*, Park *et al.* 1994). As we push to larger redshift, we must first characterize the redshift dependence of the intrinsic properties of galaxies. Only then can we compute with confidence the clustering statistics of samples that are either homogeneous in their clustering properties or that have known dependence of clustering on galaxy species. Computing the requisite multivariate luminosity functions and spectral evolution of galaxies requires multiband photometry and homogeneous samples with good resolution spectra. The SDSS will provide both of these desiderata.

5.3. CLUSTERING EVOLUTION

Clustering of galaxies fails to be ergodic as we probe deeper into the universe for yet another reason: the pattern of clustering itself evolves with time. In linear theory, the growing-mode perturbations grow with the scale factor a of the universe such that $P(k, a) \propto D^2(a)$, where $D(a)$ is a function of the cosmic matter density Ω_M and cosmological constant Ω_Λ . Relative to the present epoch, when $D(z) \equiv 1$, the growth factor when the universe had relative scale size $a \equiv (1+z)^{-1}$ is (Carroll, Press, & Turner 1992)

$$\begin{aligned}
 D(a) &= \frac{5}{2} \frac{\Omega_M}{a} \left[1 + \Omega_M \left(\frac{1}{a} - 1 \right) + \Omega_\Lambda (a^2 - 1) \right]^{1/2} \\
 &\times \int_0^a \left[1 + \Omega_M \left(\frac{1}{a'} - 1 \right) + \Omega_\Lambda (a'^2 - 1) \right]^{-3/2} da'.
 \end{aligned}
 \tag{7}$$

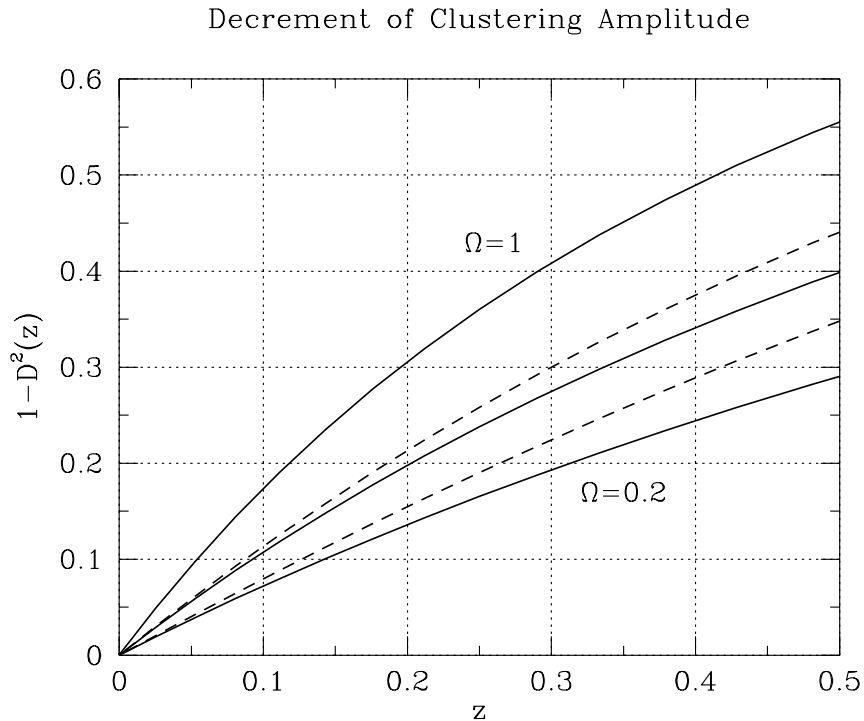


Figure 11. Evolution of the clustering amplitude with redshift for (top to bottom) $\{\Omega_M = 1, \Omega_\Lambda = 0\}$, $\{\Omega_M = 0.4, \Omega_\Lambda = 0.6\}$, $\{\Omega_M = 0.4, \Omega_\Lambda = 0\}$, $\{\Omega_M = 0.2, \Omega_\Lambda = 0.8\}$, and $\{\Omega_M = 0.2, \Omega_\Lambda = 0\}$. Plotted here is the difference in clustering amplitude relative to $z = 0$.

For $\Omega_M = 1$ and $\Omega_\Lambda = 0$, this relation is simply $D(z) = (1 + z)^{-1}$.

Figure 11 plots the apparent decrement of clustering amplitude relative to $z = 0$, $D^2(z = 1) - D^2(z) = 1 - D^2(z)$, for a few choices of spatially flat and open cosmologies. By redshift $z = 0.2$, the decrement is 30% for $\Omega_M = 1$ and 12% for an $\Omega_M = 0.2$ open universe. The difference in the decrement for these models is then larger than the statistical errors in the power spectrum on most scales for a SDSS sample to this depth.

In other words, the cosmology-dependence of the growth factor becomes the dominant source of uncertainty in estimation of the power spectrum and we reach a fundamental limit on our ability to measure the power spectrum in a model-independent fashion. This is not a problem when comparing with models that specify the cosmology, because one simply

predicts the power spectrum that would be observed over the specified volume for each model. But it is not possible to compare local measures of clustering with observations at larger redshift without specifying the cosmology. For example, apparent variation in the clustering amplitude of a galaxy species that are due to galaxy evolution might be degenerate with variation of the cosmology. Thus ends the “present epoch” for the purpose of statistical large-scale structure.

On the other hand, given the large divergence of clustering amplitude for models that might otherwise match at $z = 0$, the strong cosmology-dependence of the growth factor seems like a powerful way to constrain Ω_M and Ω_Λ . Given all of the caveats above regarding galaxy evolution, we must find a sample of objects that (1) has negligible (or, at least, very well understood) intrinsic evolution out to a redshift of a few tenths (2) are sufficiently numerous that shot noise does not dominate over the cosmic variance, and for which we (3) can easily obtain redshifts (either spectroscopic or photometric). One must use a single volume-limited sample, because the decrease of clustering amplitude with redshift might be masked by the effects of luminosity bias (brighter galaxies cluster more strongly) in a magnitude-limited sample. A good candidate for such an analysis will be the BRG sample of the SDSS, which will extend to $z = 0.45$. The brightest, reddest galaxies evolve the least and have strong spectral features that ease redshift determination for these objects. Dividing this redshift sample into broad bins of redshift and averaging the power estimates over broad bands should allow determination of the clustering amplitude to within a few percent at each redshift.

6. CONCLUSIONS

The large sample volume and dense sampling of the galaxy distribution in the SDSS redshift survey will set lower bounds to the uncertainties that could, in principle, allow detection of small deviations from smooth spectra and easily differentiate between similar cosmological models. Clever use of the anisotropy of clustering would allow simultaneous estimation of both Ω_M and the real-space power spectrum. Further, we could use the growth rate of clustering to constrain Ω_M and Ω_Λ in a different way. However, all of these dreams hinge on our ability to cleanly separate true galaxy clustering from contamination by extinction and photometric error, and to differentiate between clustering evolution and evolution of the galaxies themselves.

Thus, the future of large-scale structure lies in studying evolution, both of galaxies and of the clustering pattern itself. This evolution is strongly species-dependent and will require estimation of multivariate luminosity

functions to interpret. In a few years' time, the SDSS, together with the 2MASS infrared survey and FIRST radio surveys, which will also cover (really, have already begun to cover) the same region of sky, will provide a database of optical, near-IR, and radio information about millions of objects and will be ideal for just this sort of investigation.

The author acknowledges the collaborative effort of many of the participants in the SDSS, in particular Andy Connolly and Alex Szalay, that contributed to the results presented in this volume. Support for this work was provided by NASA through grant HF-01078.01-94A from the Space Telescope Science Institute, which is operated by AURA, Inc. under NASA contract NAS5-26555,

References

- Bardeen, J.M., Bond, J.R., Kaiser, N., & Szalay, A.S. 1986, ApJ, 304, 15.
Baugh, C.M., & Efstathiou, G. 1993, MNRAS 265, 145.
Burstein, D., & Heiles, C. 1982, AJ, 87, 1165.
Carroll, S.M., Press, W.H., & Turner, E.L. 1992, ARAA, 30, 499.
Colless, M. 1998, Phil. Trans. R. Soc. Lond. A, submitted (preprint astro-ph/9804079).
Connolly, A.J., Csabai, I., Szalay, A., Koo, D.C., Kron, R.G., & Munn, J.A. 1995, AJ, 110, 2655.
da Costa, L.N., *et al.* 1994, ApJ, 424, L1.
da Costa, L.N., Vogeley, M.S., Geller, M.J., Huchra, J.P., & Park, C. 1994, ApJL 437, 1.
Eisenstein, D.J., & Hu, W. 1998, ApJ, 496, 605.
Feldman, H., Kaiser, N., & Peacock, J. 1994, ApJ 426, 23.
Fisher, K.B., Davis, M., Strauss, M.A., Yahil, A., & Huchra, J.P. 1993, ApJ 402, 42.
Fisher, K.B., Huchra, J.P., Davis, M., Strauss, M.A., Yahil, A., & Schlegel, D. 1995, ApJSuppl, 100, 69.
Geller, M.J., & Huchra, J.P. 1989, Science 246, 897.
Giovannelli, R., & Haynes, M.P. 1984, AJ, 89, 1.
Gunn, J.E. & Weinberg, D.H. 1995, in Wide Field Spectroscopy and the Distant Universe, proc. of 35th Herstmonceux Conf., eds. S.J. Maddox and A. Aragón-Salamanca, 3.
Hamilton, A.J.S. 1998, this volume, pp 185-274.
Kaiser, N. 1987, MNRAS, 227, 1.
Landy, D.S., Shectman, S.A., Lin, H., Kirshner, R.P., Oemler, A.A., & Tucker, D. 1996, ApJL 456, 1.
Lilly, S.J., Tresse, L., Hammer, F., Crampton, D. & Le Fevre, O., 1995, ApJ, 455, 108.
Lin, H., Kirshner, R.P., Shectman, S.A., Landy, S.D., Oemler, A., Tucker, D.L., & Schechter, P.L. 1995, ApJ, 471, 617.
Park, C., Vogeley, M.S., Geller, M.J., & Huchra, J.P. 1994, ApJ 431, 569.
Peacock, J.A. 1997, MNRAS, 284, 885.
Peacock, J.A., & Nicholson, D. 1991, MNRAS, 253, 307.
Primack, J.R., Holtzman, J., Klypin, A., & Caldwell, D.O. 1995, Phys. Rev. Lett., 74, 2160.
Saunders, W., Rowan-Robinson, M., Lawrence, A., Efstathiou, G., Kaiser, N., Ellis, R.S., & Frenk, C.S. 1990, MNRAS, 242, 318.
Saunders, W. *et al.* 1994, in Wide Field Spectroscopy and the Distant Universe, proc. of 35th Herstmonceux Conference, eds. S.J. Maddox and A. Aragón-Salamanca, 88.
Schlegel, D.J., Finkbeiner, D.P., & David, M. 1998, ApJ, 499, in press.
Shectman, S.A., Landy, S.D., Oemler, A., Tucker, D.L., Lin, H., Kirshner, R.P., & Schechter, P.L. 1996, ApJ 470, 172.

- Stark, A.A., Gammie, C.F., Wilson, R.W., Bally, J., Linke, R.A., Heiles, C., & Hurwitz, M. 1992, *ApJS*, 79, 77.
- Szalay, A.S. 1998, this volume, pp 277-289.
- Tadros, H., & Efstathiou, G. 1995, *MNRAS*, 276, L45.
- Tegmark, M., Hamilton, A.J.S., Strauss, M.A., Vogeley, M.S., & Szalay, A.S. 1998, *ApJ*, 499, 555.
- Vogeley, M.S., & Connolly, A.J. 1998, in preparation.
- Vogeley, M.S., & Szalay, A.S. 1996, *ApJ*, 465, 34.
- Wright, E.L., Bennett, C.L., Gorski, K., Hinshaw, G., & Smoot, G.R. 1996, *ApJL*, 464, L21.